



Decadal Atlantic Meridional Overturning Circulation slowing events in a climate model

M. Latif^{1,2} · T. Park^{1,3} · W. Park¹

Received: 16 August 2018 / Accepted: 16 January 2019 / Published online: 13 April 2019
© Springer-Verlag GmbH Germany, part of Springer Nature 2019

Abstract

There is a controversy about the origin of the recent decadal Atlantic Meridional Overturning Circulation (AMOC) slowing observed at 26.5°N and concurrent sea surface temperature cooling in the central and eastern mid-latitude North Atlantic. We investigate decadal AMOC slowing events simulated in a multi-millennial preindustrial control integration of the Kiel Climate Model (KCM), providing an estimate of internal AMOC variability. Preindustrial control integrations of 15 models participating in the Coupled Model Intercomparison Project phase 5 also are investigated, as well as historical simulations with them providing estimates of AMOC variability during 1856–2005. It is shown that the recent decadal AMOC decline is still within the range of the models' internal AMOC variability and thus could be of natural origin. In this case, the decline would represent an extreme realization of internal variability provided the climate models yield realistic levels of AMOC variability. The model results suggest that internal decadal AMOC variability is large, requiring multi-decadal observational records to detect an anthropogenic AMOC signal with high confidence. When analyzing the strongest decadal AMOC slowing events in the KCM, which have amplitudes similar to or larger than the recently observed decadal AMOC decline, the following composite picture emerges: a very strong decadal AMOC decline is preceded by a decadal rise in atmospheric surface pressure over large parts of the mid-latitude North Atlantic. The change in low-level atmospheric circulation drives reduced oceanic heat loss over and diminished upper-ocean salt content in the Labrador Sea. In response, oceanic deep convection and subsequently the AMOC and northward oceanic heat transport weaken, and anomalously cold sea surface temperatures develop in the central and eastern mid-latitude North Atlantic.

1 Introduction

The Atlantic Meridional Overturning Circulation (AMOC) is a major oceanic current system with potentially widespread climate impacts (Sutton and Hodson, 2005; Levermann et al. 2005; McCarthy et al. 2015a, b; Goddard et al. 2015). Many climate models project a significant AMOC slowing during the twenty first century in response to an accelerated global warming should atmospheric greenhouse gas concentrations continue to rise unabatedly (Schmittner et al. 2005; Reintges et al. 2017). The Earth's globally

averaged surface air temperature (SAT) already rose by approximately 1 °C since 1880, which to a large extent has been attributed to anthropogenic greenhouse gas emissions (Bindoff et al. 2013). There is significant regional variation in the surface warming pattern. For example, the centennial sea surface temperature (SST) trend pattern calculated over the twentieth century contains a warming hole over the North Atlantic, which has been interpreted in a recent study as a long-term AMOC slowing (Caesar et al. 2018). However, there is some debate about the cause of the warming hole. By means of climate models employing observed external forcing (Cheng et al. 2013; Bindoff et al. 2013), the warming hole has been attributed on the one hand to a slowing of the AMOC (Drijfhout et al. 2012) and on the other hand to anthropogenic aerosol emissions and periods of volcanic activity (Booth et al. 2012). The latter explanation has been criticized by Zhang et al. (2013) because of major discrepancies between the simulations and observations, for example with regard to North Atlantic upper-ocean heat content. Internal, i.e. unforced AMOC variability

✉ M. Latif
mlatif@geomar.de

¹ GEOMAR Helmholtz Centre for Ocean Research Kiel, Kiel, Germany

² Excellence Cluster "Future Ocean", Kiel University, Kiel, Germany

³ Korea Polar Research Institute, Incheon, Korea

possibly also could explain the warming hole over the North Atlantic, since some climate models simulate pronounced multi-decadal to multi-centennial AMOC variability in control integrations without time-dependent external forcing (Delworth et al. 1993; Park and Latif 2008; Delworth and Zeng 2012). The long-term internal AMOC variability simulated in the models is associated with changes in the northward oceanic heat transport, which in turn is reflected in North Atlantic SST.

Recently, a marked decadal decline in the AMOC strength and oceanic poleward heat transport has been observed at 26.5°N (Cunningham et al. 2013; Bryden et al. 2014; Smeed et al. 2014; Srokosz and Bryden 2015), which was followed by anomalously low SST in the central and eastern mid-latitude North Atlantic (Fig. 1a). The underlying mechanism of this recent decadal AMOC decline is still under debate; and both internal and external factors have been proposed. Nigam et al. (2018) report decadal pulses within the lower-frequency Atlantic Multidecadal Oscillation (AMO), representing decadal variability of the subpolar gyre, which originate from meridional excursions of the Gulf Stream and sectional detachments. Variations in the density of deep waters in the Labrador Sea have been suggested as a useful predictor of changes in the AMOC (Robson et al. 2013), and the recent AMOC slowing has been linked to record-low densities in the deep Labrador Sea (Robson et al. 2016). On the contrary, observations from a 17-year long mooring array at the exit of the Labrador Sea at 53°N, monitoring the transport of the Deep Western Boundary Current which is part of the cold water path of the AMOC, depict a wide range of variability but no sustained long-term trend (Handmann et al. 2018).

Can some of the recent observations, in particular the decadal AMOC decline at 26.5°N, be interpreted in the context of an anthropogenic AMOC slowing or does the decline simply reflect natural AMOC variability? This is a challenging question, as the AMOC strongly varies naturally on a wide range of timescales, which can be concluded on the basis of forced ocean model and of climate model simulations, ocean syntheses, SST observations during the instrumental record, and direct current measurements covering about the last two decades (Park and Latif 2008; Delworth and Zeng 2012; Iwi et al. 2012; Park and Latif 2012; Dima and Lohmann 2010; Ritz et al. 2013; Srokosz and Bryden 2015; McCarthy et al. 2015a, b; Pohlmann et al. 2013; Swingedouw et al. 2015; Jackson et al. 2016; Handmann et al. 2018). Here we estimate by means of a version of the Kiel Climate Model (KCM) and a number of models participating in the Coupled Model Intercomparison Project phase 5 (CMIP5) the level of internal decadal AMOC variability in the model world and put the recent decadal AMOC slowing at 26.5°N into perspective with the models' variability. Further, we compare, as far as possible, the spatial patterns of selected quantities, which have been observed in association with the recent decadal AMOC slowing, with the model patterns and also use analysis/reanalysis products for the comparison. The intention of this study is twofold: first, we address the question as to whether the observed decadal AMOC decline at 26.5°N is within range of natural variability simulated by the climate models. Second, we derive a physical picture of how strong decadal AMOC slowing events are generated internally in the KCM and evaluate to which extent the derived mechanism could explain the

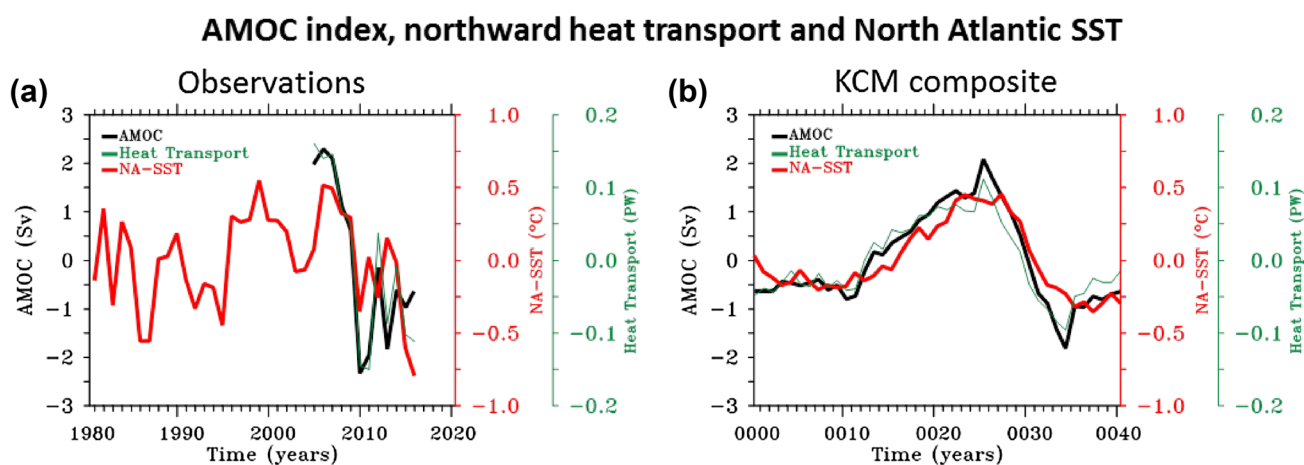


Fig. 1 Anomalies of the AMOC strength (Sv, black) and oceanic northward heat transport (PW, green) at 26.5°N, and North Atlantic (NA) SST (°C, red) averaged over 50°W–10°W, 40°N–55°N (box in Fig. 5c). **a** Observations: AMOC strength and oceanic northward heat transport during April 2004–October 2015 from RAPID, and

NA SST from HadISST during 1980–2015. **b** Composite evolution derived from the Kiel Climate Model (KCM) by averaging over the 26 decadal AMOC slowing events simulated in a multi-millennial control integration of the model that exceed two standard deviations of the decadal AMOC trend distribution (Fig. 2b)

recent decadal AMOC slowing and concurrent changes in other quantities.

The paper is organized as follows. Section 2 introduces the KCM and the CMIP5 models, and describes the applied methodology. The main results are presented in Sect. 3. A summary and discussion of the major results are given in Sect. 4 and conclude the paper.

2 Climate models, data and methods

We use in this study a version of the KCM which was described originally in detail by Park et al. (2009). The KCM version used here (Park et al. 2016) consists of the ECHAM5 atmosphere general circulation model (AGCM) on a T42 ($2.8^\circ \times 2.8^\circ$) grid and with 19 vertical levels coupled to the NEMO ocean-sea ice GCM on a 2° Mercator mesh with 0.5° meridional resolution in the equatorial region and 31 vertical levels. A surface freshwater correction is applied to the model over the North Atlantic, which leads to a much improved mean horizontal ocean circulation in the North Atlantic, a stronger AMOC and related poleward heat transport, and an enhanced multi-decadal AMOC and Northern Hemisphere SAT variability relative to the uncorrected model version (Park et al. 2016). In particular, the cold SST bias over the North Atlantic, a common feature of many climate models employing coarse-resolution ocean models, is much reduced by the application of the surface freshwater correction. The state of the North Atlantic subsurface ocean down to about 1 km as well is considerably improved by the surface freshwater flux correction. We analyze a multi-millennial preindustrial control integration of this KCM version, employing constant atmospheric CO_2 -concentration of 286 parts per million (ppm).

We additionally use preindustrial control integrations and historical simulations employing observed radiative forcing with 15 models participating in the Coupled Model Inter-comparison Project phase 5 (CMIP5; Taylor et al. 2012). The CMIP5 models are: ACCESS1.3, CanESM2, CCSM4, CNRM-CM5, FGOALS-s2, GFDL-CM3, GFDL-ESM2M, GISS-E2-R, MIROC5, MPI-ESM-LR, MPI-ESM-MR, MPI-ESM-P, MRI-CGCM3, NorESM1-ME, and NorESM1-M. We selected 150 years from the preindustrial control integrations and historical simulations (1856–2005).

We investigate a number of atmospheric and oceanic variables from the following datasets: NCEP Reanalysis products (1980–2014) for sea level pressure and surface heat flux are provided by the National Oceanographic and Atmospheric Administration (<https://www.esrl.noaa.gov/psd/data/gridded/>). We note that surface heat fluxes from NCEP Reanalysis are subject to large uncertainties (Sun et al. 2003). For SST we use data from HadISST provided by UK Met Office (<http://www.metoffice.gov.uk/hadobs/hadisst/>).

Altimetry dynamic sea level data are from Ssalto/Duacs and distributed by AVISO (<http://www.aviso.altimetry.fr/duacs/>). Atlantic meridional overturning data from 26.5°N are from the RAPID-MOCHA-WBTS program available at <http://www.rapid.ac.uk/rapidmoc>. EN4.1.1 ocean analysis data are used for subsurface temperatures and salinities to calculate upper ocean (0–700 m) heat content and salt content and obtained from UK Met Office (<http://www.metoffice.gov.uk/hadobs/en4/>). For ocean heat content and mixed layer depth (MLD), Simple Ocean Data Assimilation (SODA) (<https://climatedataguide.ucar.edu/climate-data/soda-simple-ocean-data-assimilation>) is used. For heat content National Oceanographic Data Center (NODC) (https://www.nodc.noaa.gov/OC5/3M_HEAT_CONTENT/) product is used along with the EN4.1.1.

Decadal AMOC trend distributions were calculated and a two-sigma threshold was applied to select the strongest decadal AMOC slowing events (see Figs. 2, 3). We consider 41 years around each event (Fig. 4). Decadal trends are defined by subtracting adjacent 5-year averages. Three 5-year averages are calculated for each of the AMOC slowing events: P1 (model years 20–24), P2 (model years 25–29) and P3 (model years 30–34). These 5-year averages are used to compute the decadal trends prior (P2–P1) and during the AMOC declines (P3–P2), respectively. The composites are based on 26 (KCM, Fig. 4) and 22 (CMIP5) decadal AMOC slowing events. Decadal-trend patterns from observations and analysis/reanalysis products were calculated in an analogous manner, i.e. by subtracting adjacent 5-year averages: P1 (2000–2004), P2 (2005–2009) and P3 (2010–2014). Statistical significance was assessed by a Student's t-test.

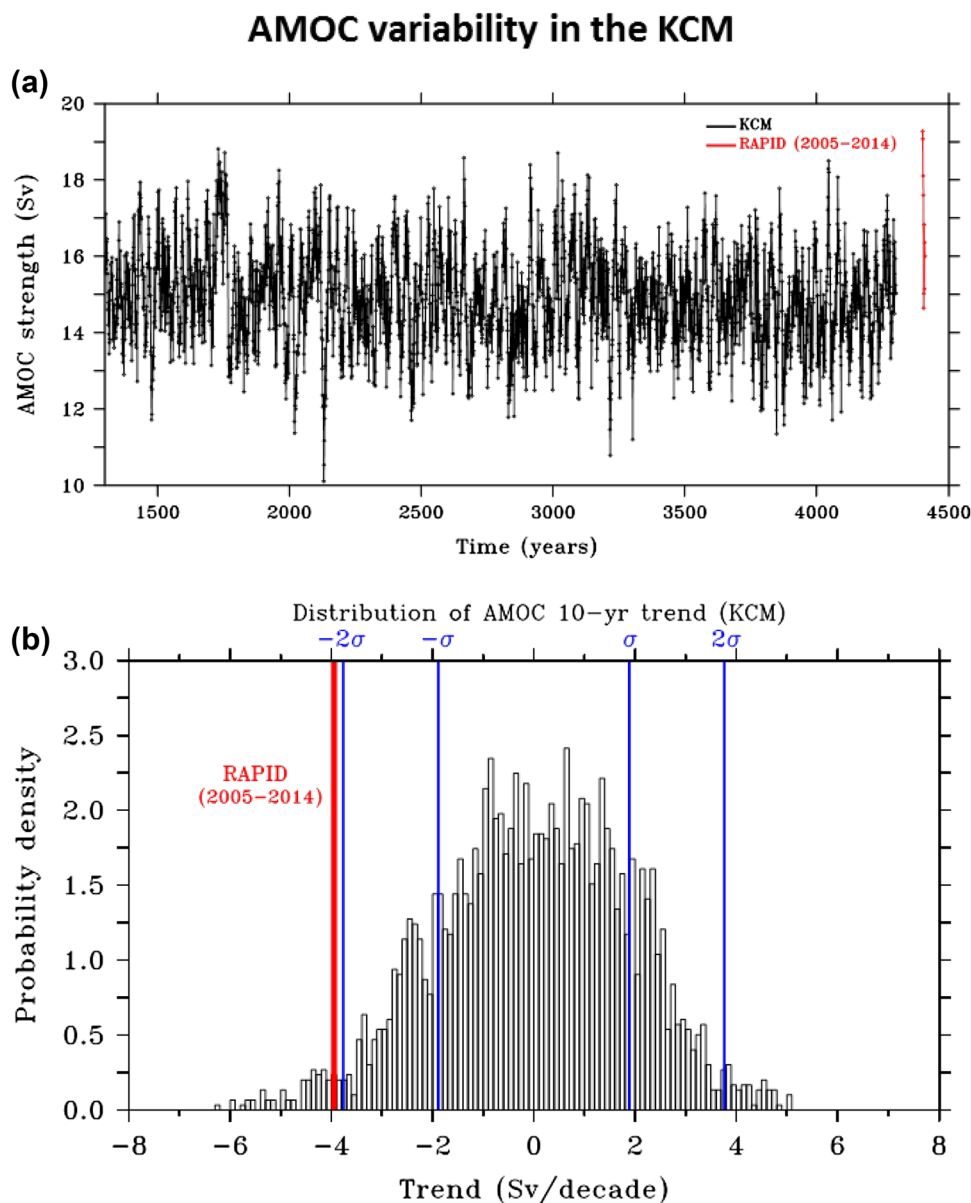
Annual data were used unless stated otherwise, and the model data were detrended prior to analysis. We note that detrending does not significantly change the decadal AMOC-trend distributions calculated from the historical simulations with the CMIP5 models.

3 Results

3.1 Assessment of the recent decadal AMOC slowing

Pronounced AMOC variability on a wide range of time-scales is observed in the multi-millennial preindustrial control integration of the KCM (Fig. 2a), including several decadal AMOC slowing events with rates exceeding that during 2005–2014. This can be inferred from the distribution of decadal AMOC trends (Fig. 2b). The most extreme decadal AMOC slowing event simulated by the KCM depicts a decline of more than 6 Sv/decade at 26.5°N . We note a negative skewness in the distribution derived from the KCM: extreme decadal AMOC slowing

Fig. 2 Pronounced AMOC variability is simulated in a multi-millennial preindustrial control integration of the KCM. **a** Annual values of the maximum overturning streamfunction (Sv) at the grid point nearest to 26.5°N (black) and the data from the RAPID array (red). **b** The distribution of non-overlapping decadal (10-year) AMOC trends (Sv/10-year) derived from the model time series shown in **a**. The vertical lines are the decadal trend (2005–2014) from RAPID (red), and the $\pm 2\sigma$ and $\pm 1\sigma$ decadal trends (blue) from the KCM. The model data were detrended prior to analysis



events can become stronger than decadal AMOC speedup events. The recent decadal AMOC decline also is within the multi-model decadal trend distributions derived from the preindustrial control integrations of (Fig. 3a) and historical simulations (Fig. 3b) with the 15 CMIP5 models.

In summary, the climate models investigated here suggest that the recent marked decadal AMOC decline could have been due to internal variability, which also has been suggested by Roberts et al. (2014) and Jackson et al. (2016). In this case, however, the recent decadal AMOC slowing would represent an extreme realization of such variability provided the climate models realistically capture the level of internal AMOC variability.

3.2 Spatial structure of trends in selected quantities linked to decadal AMOC slowing events

Many realizations of extraordinarily strong decadal AMOC slowing events can be analyzed from the preindustrial control integration of the KCM (Fig. 4), which allows identifying common behavior among as well as variation across the decadal AMOC slowing events. The composite-time evolutions of the AMOC strength and oceanic northward heat transport at 26.5°N as well as the mid-latitude North Atlantic SST east of 50°W (Fig. 1b), as calculated from the 26 decadal AMOC slowing events exceeding the 2σ -threshold, are

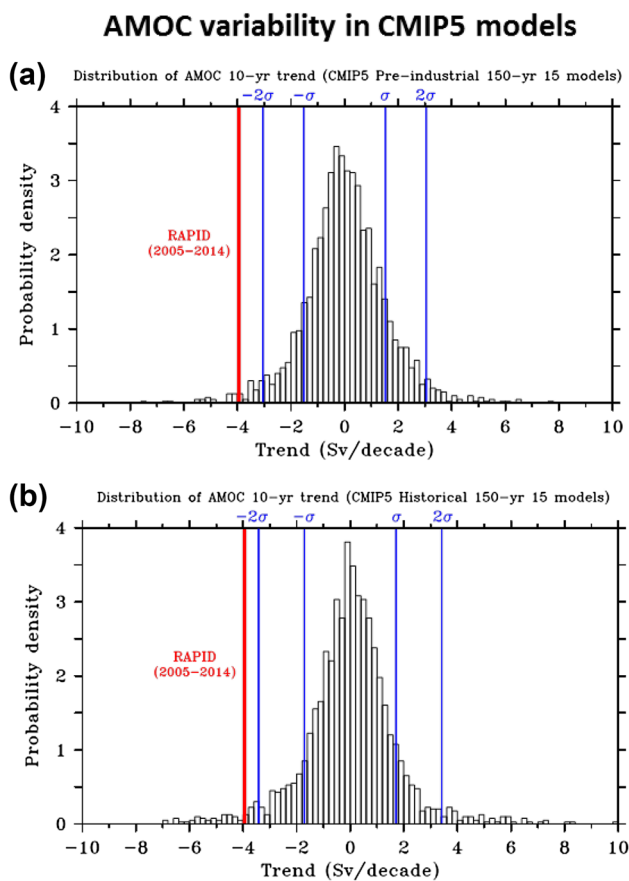


Fig. 3 The distribution of non-overlapping decadal (10-year) AMOC trends (Sv/10-year) computed from the 15 CMIP5 models. **a** Calculated from the preindustrial control integrations, **b** calculated from the historical simulations employing observed external forcing. The vertical lines are the decadal trend from RAPID (red), and the $\pm 2\sigma$ and $\pm 1\sigma$ decadal trends from the model ensemble (blue). The model data were detrended prior to analysis

consistent with the observed evolutions during 2005–2014 with respect to amplitude and phasing (Fig. 1a). This supports the notion that the strongest decadal AMOC slowing events in the model exhibit aspects that also played a role in the recently observed AMOC decline.

We now turn to the spatial trend patterns of selected variables that are associated with decadal AMOC slowing events. First, the decadal trend patterns derived from observations and analysis/reanalysis products during the decadal AMOC slowing of 2005–2014 are briefly described (Fig. 5, left panels). A decadal rise in sea level pressure (SLP) during 2000–2009, centered near 45°N and 30°W (Fig. 5a), preceded the AMOC slowing. The SLP trend pattern does not project well on the North Atlantic Oscillation (NAO; Hurrell 1995) and shares some similarities with the East Atlantic Pattern (EAP; Barnston and Livezey 1987). Decadal trends shifted by 5 years, representing changes during 2005–2014, depict a cooling of mid-latitude North Atlantic

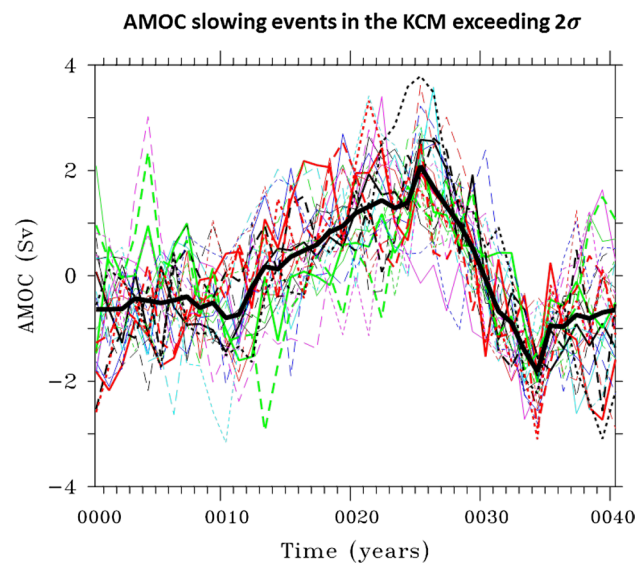


Fig. 4 The KCM simulates a number of rather strong decadal AMOC slowing events. Shown are the 26 events (Sv) exceeding the 2σ -threshold depicted in Fig. 2b. The composite evolution is calculated by averaging over these 26 AMOC slowing events and shown by the solid black line

SST east of 50° W and warming off the coast of North America (Fig. 5c). In climate models, this kind of a dipolar SST change pattern is often linked with a weakening of the AMOC, a connection which also is supported by proxy data (Saba et al. 2016). Sea surface height (SSH, Fig. 5e) from satellites and upper ocean (0–700 m) heat content (OHC) from 3 products (Fig. 6a–c) imply pronounced horizontal ocean circulation changes during 2005–2014: a northward displacement of the Gulf Stream, as described by Nigam et al. (2018) discussing decadal pulses in the AMO during 1954–2012 by means of ocean surface and subsurface salinity and temperature observations, and an eastward expansion of the subpolar gyre. Differences among the OHC products are obvious but the large-scale features robust. Changes in net surface heat flux (Q_{net} , Fig. 5g) during 2005–2014 are mostly out of phase with the SST changes, suggesting that the latter are primarily driven by ocean dynamical processes.

Next, the decadal-trend composites are discussed that have been calculated from the 26 strongest decadal AMOC slowing events simulated in the preindustrial control integration of the KCM (Fig. 5, right panels). We note that significant model-data differences are to be expected, because a single event, as the decadal AMOC decline during 2005–2014, is potentially more influenced by the effects of atmospheric or oceanic noise than a composite which provides the evolution averaged over many decadal AMOC slowing events, in which the influence of the noise is strongly damped. We note in this context that the coarse-resolution of the ocean model used in the KCM largely

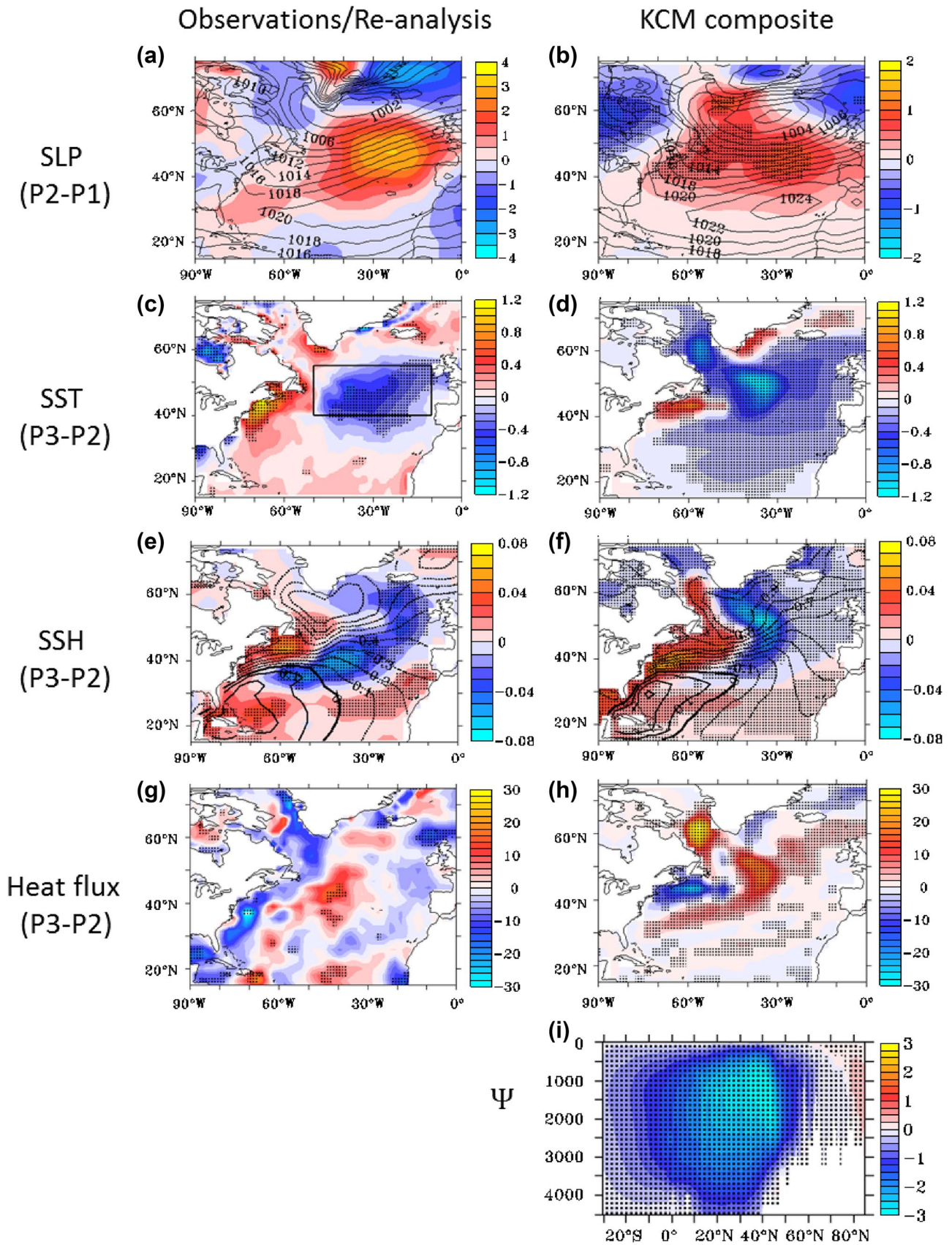


Fig. 5 **a** SLP differences (hPa) P2 (2005–2009) minus P1 (2000–2004) from NCEP, **b** KCM composite. **c** SST differences (K) P3 (2010–2014) minus P2 (2005–2009) from HadISST, **d** KCM composite. **e** SSH differences (m, global average removed) P3-P2 from AVISO, **f** KCM composite. **g** Net surface heat flux differences (W m^{-2} , positive values indicate flux into the ocean) P3-P2 from NCEP, **h** KCM composite. **i** KCM overturning streamfunction composite (Sv). Contours in **a**, **b**, **e**, **f** depict long-term climatology. Dotted regions indicate areas which are significant at the 90%-level

inhibits the generation of chaotic ocean variability as that linked to mesoscale eddies. Thus the noise in the KCM is basically due to chaotic weather fluctuations. The influence of the noise is reflected among others in the statistical significance: while only limited regions in the trend patterns associated with the recent decadal AMOC decline, which have been derived from observations and analysis/reanalysis products, exhibit statistical significance at the 90% level, the model's composite-trend patterns linked to the 26 strongest decadal AMOC declines exhibit statistical significance over large regions.

Prior (P2-P1) to major decadal AMOC slowing events in the KCM, on average a decadal rise in SLP is simulated over most of the mid-latitude North Atlantic (Fig. 5b), somewhat similar to the decadal SLP-trends observed during 2000–2009 (Fig. 5a). The composite decadal-SST trends shifted by 5 years (P3-P2) relative to the SLP trends (P2-P1) depict cooling over large parts of the mid-latitude North Atlantic and warming off the coast of North America (Fig. 5d), which also is consistent with the observations (Fig. 5c). A rather similar decadal SST-trend composite is obtained from the preindustrial control integrations of the 15 CMIP5 models (Fig. 7), which has been computed in an analogous manner as that from the KCM, i.e. by applying the 2σ -threshold to the decadal AMOC-trend distribution to select the events (Fig. 3a).

The decadal trend composites (P3-P2) of SSH (Fig. 5f) and OHC (Fig. 6d) calculated from the KCM, like the data, imply changes in the horizontal ocean circulation. A common feature among the model and the data is the dipolar pattern in SSH and OHC with positive signals in the western North Atlantic off the coast of North America and negative signals in the central North Atlantic stretching in a northeastern direction. The composite-decadal trends (P3-P2) in the net surface heat flux (Q_{net} , Fig. 5h) is in opposite phase with the SST trends (Fig. 5d), indicating that the decadal SST changes in the KCM, linked to strong decadal AMOC slowing events, are mostly driven by ocean dynamical processes. The decadal trend composite (P3-P2) of the overturning stream function Ψ (Fig. 5i) derived from the KCM indicates a basin-wide weakening of the North Atlantic Deep Water Cell.

3.3 Role of noise in biasing decadal SST trends

As mentioned above, a “perfect” match between the observed changes, which represent a single realization of decadal variability, and the composite decadal-trend maps cannot be expected given the large noise level in the mid-latitudes. For example, major differences with respect to the decadal SST trends are seen over the Labrador Sea: while the observations depict weak warming or no change in SST (Fig. 5c), the KCM on average simulates surface cooling (Fig. 5d). The decadal SST-trend composite calculated from the CMIP5 models also depicts cooling over the Labrador Sea (Fig. 7). We hypothesize that the model-data differences in the SST over the Labrador Sea are due to weather noise, specifically the exceptional but short-lived drop in the winter-NAO index during 2009–2010 (Jung et al. 2011), keeping in mind that the annual-mean NAO index is dominated by the winter-mean index. A negative phase of the winter-NAO index is generally associated with warming SSTs over the Labrador Sea due to reduced oceanic heat loss mainly forced by diminished cold air advection from the north. The exceptional drop in the winter-NAO index during 2009–2010 also would explain the warming SSTs observed over the subtropical North Atlantic, as a negative NAO-phase is associated with anomalously weak trade winds in this region that drive a reduction in evaporation from and warming of the sea surface. In contrast, the KCM and the CMIP5 models, when averaging over the strongest decadal AMOC declines, simulate cooling SSTs over most of the trade wind region.

Each of the major decadal AMOC slowing events derived from the KCM evolves differently, as exemplified by the individual AMOC indices (Fig. 4). The spatial trend patterns associated with each of the decadal AMOC declines also considerably differ among realizations. To demonstrate the influence of the noise on the decadal SST-trend maps we have chosen 3 out of the 26 AMOC slowing events from the KCM, which exhibit warming over the Labrador Sea (Fig. 8, bottom panels). As shown above, the composite decadal SST-trend map calculated by averaging over all 26 cases (Fig. 5d) features an SST cooling in this region as does the multi-model decadal SST-trend composite pattern calculated from the 15 CMIP5 models (Fig. 7). The three realizations from the KCM indicate that the individual decadal SST-trend patterns can largely differ from each other and from the composite-trend pattern (Fig. 5d), although, by definition, all realizations are linked to a very strong decadal AMOC slowing event. The situation can be compared to the El Niño/Southern Oscillation (ENSO). Individual El Niño events, for example, come in different flavors with regard to the spatial SST anomaly pattern, but all El Niño events are preceded by a buildup of equatorial heat content.

In the top panels of Fig. 8, we show the annual SLP anomalies during model years 29–30 (which would

Upper-ocean heat content

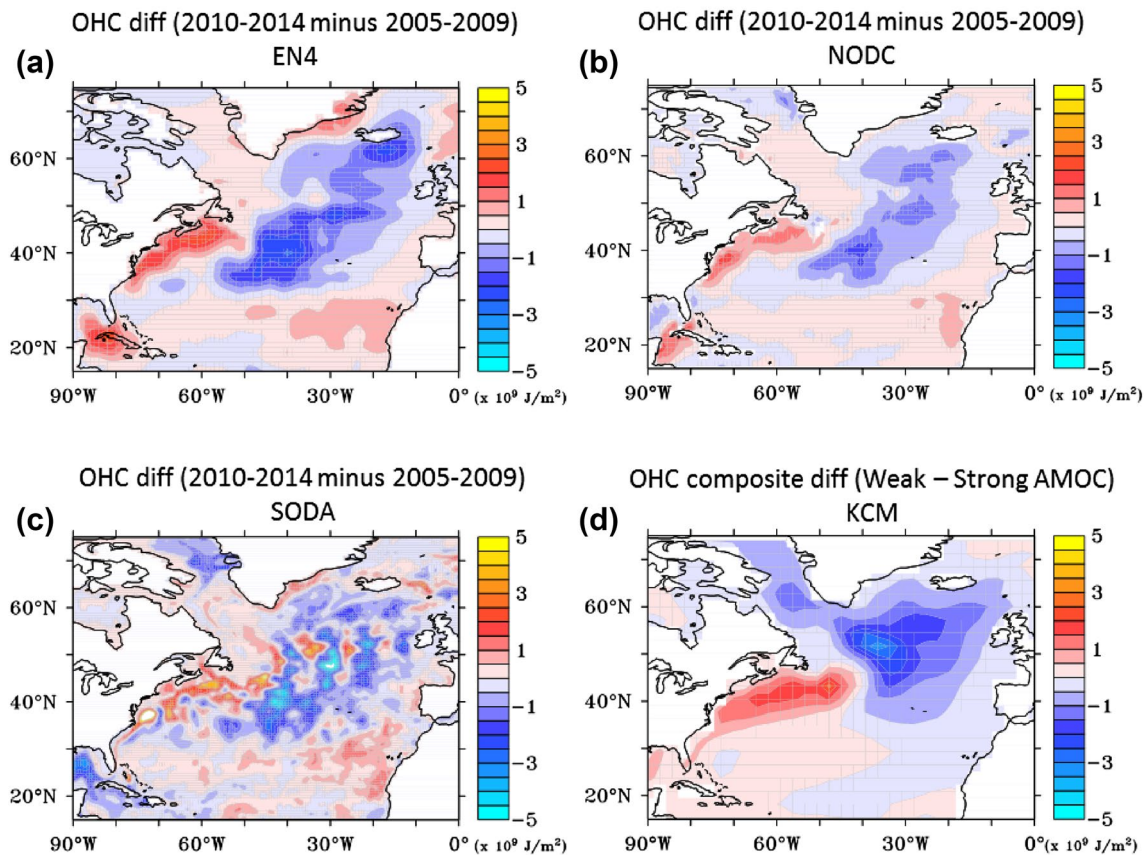


Fig. 6 Upper (0–700 m) ocean heat content (OHC, 10^9 J/m^2) differences between 5-year averages around decadal AMOC slowing. **a–c** OHC differences between 2010–2014 and 2005–2009 from EN4,

NODC and SODA, respectively. **d** OHC composite differences from the KCM. Differences between P3 and P2 are shown

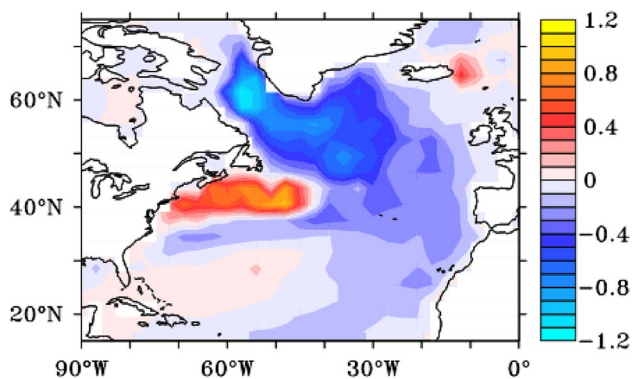


Fig. 7 SST composite differences ($^{\circ}\text{C}$) calculated from the decadal AMOC slowing events exceeding two standard deviations of the decadal AMOC variability simulated in preindustrial control integrations (Fig. 3a) of the models participating in the Coupled Model Intercomparison Project phase 5 (CMIP5). Differences between P3 and P2 are shown

correspond to years 2009–2010 in the observations), which is in the middle of the composite-AMOC decline (Fig. 1b), for each of the three decadal AMOC-slowness events which exhibit surface warming over the Labrador Sea (Fig. 8, bottom panels). The annual SLP anomalies have been calculated relative to the 41-year mean of each event. Although all three annual SLP anomalies differ from each other, they have one element in common: a less intense Icelandic low. The implied low-level atmospheric circulation anomaly has a southerly component over the Labrador Sea, which would hinder cold air advection from the north, thereby explaining the surface warming over the Labrador Sea. This supports our hypothesis, put forward above, that the large drop in the winter-NAO index during 2009–2010 and the associated changes in the oceanic heat loss biased the decadal SST trend over the Labrador Sea. The above considerations suggest that decadal SST trends over the North Atlantic are strongly affected by short-term atmospheric noise not well suited to monitor decadal AMOC variability. We note that this statement

Three Labrador Sea warming cases from the 26 AMOC slowing events

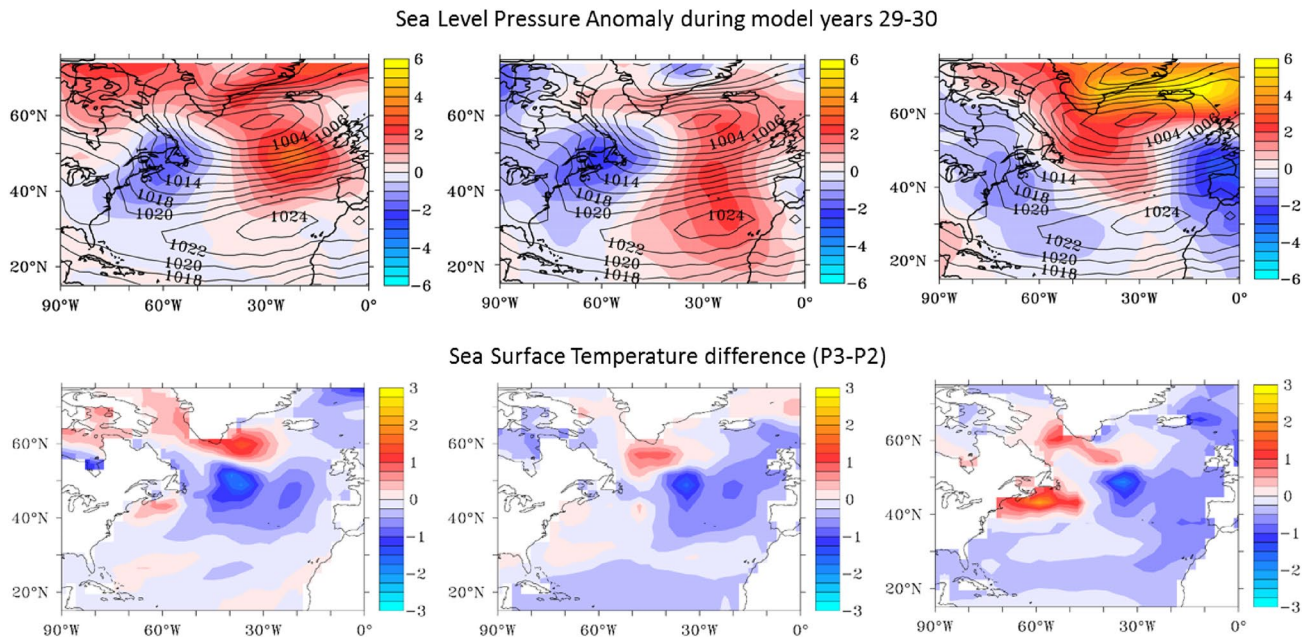


Fig. 8 Short-term atmospheric fluctuations can bias SST trends linked to decadal AMOC-slowing events. Three decadal AMOC slowing events taken from the multi-millennial control integration of the KCM are considered. Top: Biennial SLP anomalies during model years 29–30 (calculated relative to the 41-year mean of each decadal

AMOC-slowing event, Fig. 4), when the rate of AMOC slowing is large. Contours depict long-term climatology. Bottom: Decadal SST-trend maps (P3-P2) from the three decadal AMOC-slowing events chosen, which all depict warming over the Labrador Sea

may not necessarily apply to AMOC variability on multi-decadal and longer timescales.

3.4 Mechanism of decadal AMOC slowing events in the KCM

The composite evolution is now used to investigate the joint aspects behind the major decadal AMOC declines in the KCM. We also do this to help interpreting the limited observations during the recently observed AMOC decline. This is justified, because, in our opinion, the model reproduces some important aspects observed during the recent AMOC decline, keeping in mind that we are comparing a model composite, based on many decadal AMOC slowing events, with a single event.

We first briefly discuss the time evolution of Labrador Sea density from the surface down to 2500 m as obtained from ocean analysis. In many climate models, Labrador Sea density is an important driver of the AMOC. We note that the density evolution from ocean analysis is quite noisy and exhibits strong interannual variability (Fig. 9a). Most prominent are the density changes in the upper ocean, but changes at mid-depth may be more important to the AMOC. Between about 500 and 1000 m, a negative density anomaly develops in the early 2000s, which leads the decline in the AMOC

index at 26.5°N. Only the salinity contribution (Fig. 9c) depicts a negative signal at mid-depth in the early 2000s. At this time, the temperature contribution (Fig. 9e) shows a negative signal above 500 m, which seems to slowly propagate downward during the following years. In the mid-2000s, the temperature contribution also becomes negative at mid-depth, so that both temperature and salinity now contribute to the reduction in density in this depth range. During the following few years, the temperature contribution remains negative with largest magnitudes from the surface down to about 700 m, while the salinity contribution becomes positive.

The composite-density evolution calculated from the KCM is rather smooth, as expected from the averaging, and also shows the largest density anomalies in the upper ocean (Fig. 9b). Negative density anomalies at mid-depth (Fig. 9b) precede the fast composite-AMOC slowing in model year 30. There is a marked difference between the salinity (Fig. 9d) and temperature (Fig. 9f) contributions to the density change at mid-depth with respect to the timing: in the model, the temperature contribution becomes negative several years earlier than the salinity contribution. As in the ocean analysis (Fig. 9e), the temperature contribution seems to originate at the surface and then slowly propagates downward.

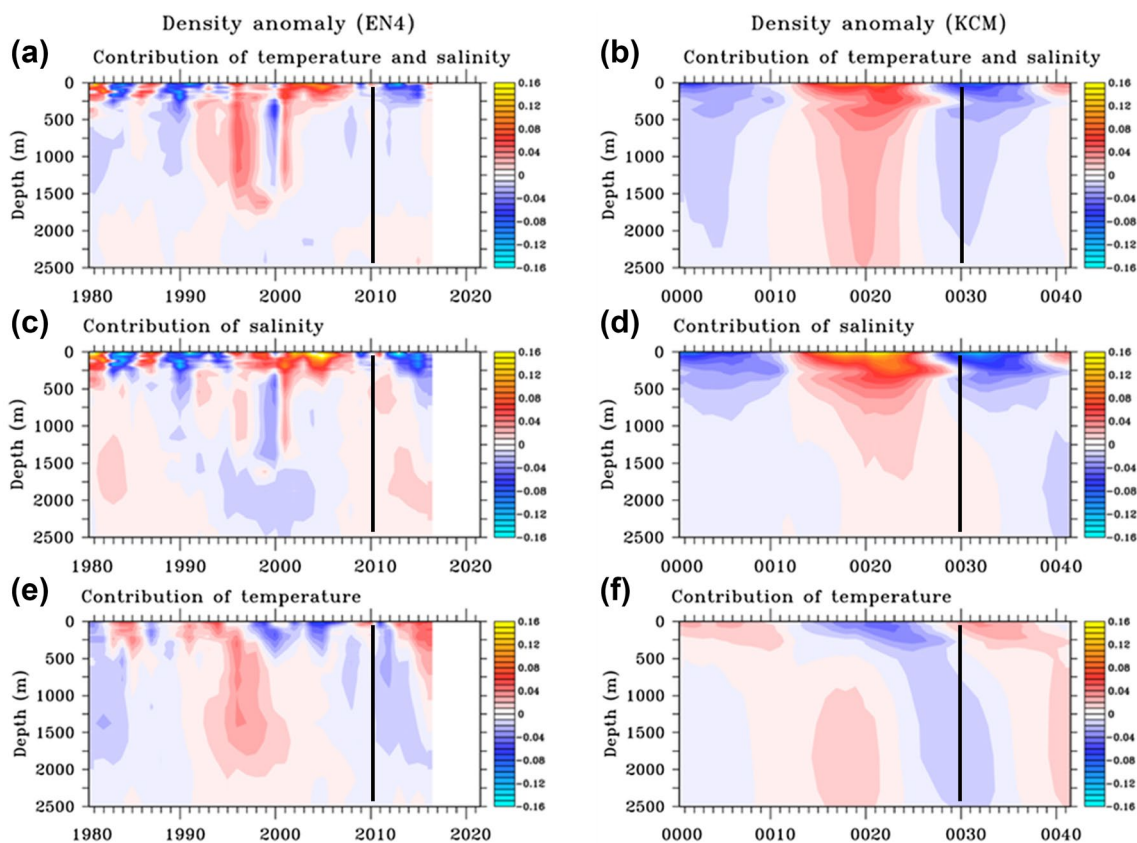


Fig. 9 a, b Anomalies of the density in the Labrador Sea (70°W – 45°W , 55°N – 70°N), and their c, d salinity and e, f temperature contributions. Left panels depict results from EN4 ocean analysis, right panels the composite time evolutions from the KCM. Den-

sity and its contributions are in units of (kg m^{-3}). The black vertical lines indicate the time of the minimum of the AMOC index at 26.5°N in the observations (left panels) and the middle of the composite-AMOC slowing from the KCM (right panels)

The picture which emerges from the KCM suggests two stages of density change at mid-depth in the Labrador Sea prior to the composite-AMOC index decline: during the first stage, which starts about 10–15 years before the AMOC slowing, a temperature-related density signal, which originates from reduced oceanic heat loss (see below), develops at the surface and slowly propagates downward. During the second stage, a few years prior to the AMOC slowing, the salinity contribution to the density change also becomes negative. Both contributions exhibit negative anomalies around model year 30. We argue that the time difference between the temperature and salinity contributions to the density change is due to the adjustment of the horizontal ocean circulation in response to the change in low-level atmospheric circulation, which alters the upper-ocean salt content (see below). The oceanic heat loss, on the other hand, responds more or less instantaneously to the change in the low-level atmospheric circulation.

We now discuss the two stages in more detail. The oceanic heat loss over the Labrador Sea is shown together with the upper ocean (0–700 m) heat content in Fig. 10. As

described above, the observations depict a decadal rise in SLP over parts of the North Atlantic prior to the AMOC decline (Fig. 5a), which implies anomalous southerly surface flow to the west of the high pressure anomaly center and thus also over the Labrador Sea. The anomalous southerlies tend to oppose the cold air advection from the north, thereby reducing the oceanic heat loss over the Labrador Sea. In fact, atmospheric reanalysis though noisy yields a decadal reduction in the oceanic heat loss over the Labrador Sea prior to the AMOC decline at 26.5°N (Fig. 10a). The composite-evolution of the oceanic heat loss over the Labrador Sea calculated from the KCM also shows a decline prior to major decadal AMOC declines (Fig. 10b). Upper-ocean (0–700 m) Labrador Sea heat content evolves basically in phase with the AMOC index, in both ocean analysis (Fig. 10c) and in the composite derived from the KCM (Fig. 10d), which is consistent with the temporal evolution of the northward heat transport at 26.5°N (Fig. 1).

We depict the evolution of the upper (0–700 m) Labrador Sea salt content in Fig. 10e, f. A drop in the upper-ocean salt content a few years prior to the AMOC decline

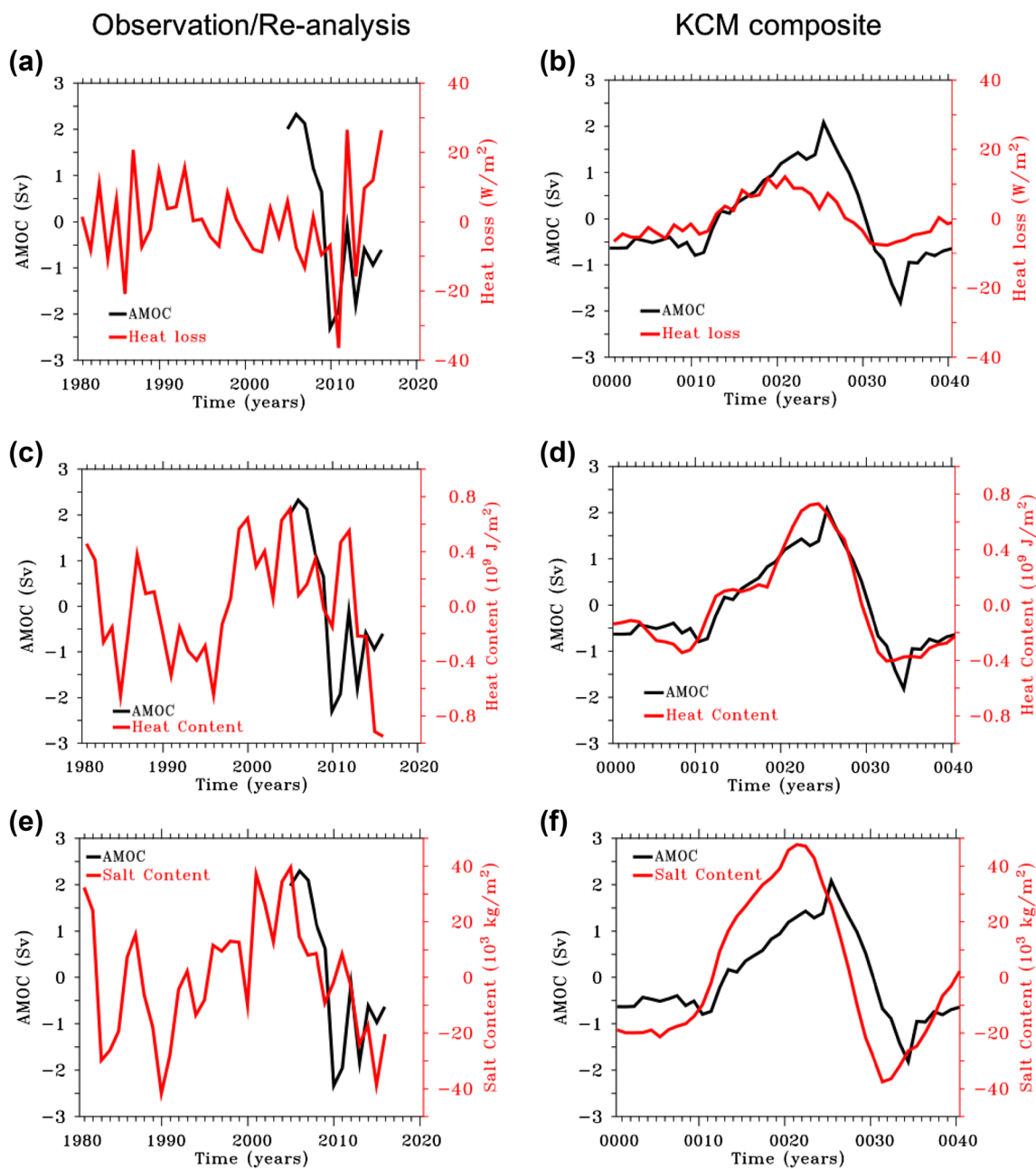


Fig. 10 Anomalies of the oceanic heat loss ($W m^{-2}$) and the upper ocean (0–700 m) heat content ($10^9 J m^{-2}$, red) and salt content ($10^3 kg m^{-2}$, red) of the Labrador Sea ($70^{\circ}W-45^{\circ}W, 55^{\circ}N-70^{\circ}N$), and of the AMOC index at $26.5^{\circ}N$ (Sv). **a** The heat loss over the Labrador

Sea from NCEP reanalysis (red) and the AMOC index from RAPID (black) and **b** composite evolutions from the KCM. The upper ocean **c** heat and **e** salt content from EN4 ocean analysis and **d, f** composite evolutions from the KCM

is inferred from ocean analysis (Fig. 10e). Consistent with this, the composite-salt content from the KCM also has a drop a few years prior to the decadal AMOC decline (Fig. 10f). The reduction in salt content must be due to dynamical processes, because the change in salt content induced by the surface freshwater flux, as derived from the KCM as well from ocean analysis, is very small (not shown).

Late-winter Labrador Sea mixed layer depth (MLD), a measure of oceanic deep convection, calculated from ocean reanalysis exhibits a decadal decline prior to the AMOC slowing but with large interannual variability superimposed (Fig. 11a). The composite-evolution of the Labrador Sea MLD calculated from the KCM is less noisy and shows a pronounced drop prior to the decline in the composite-AMOC index (Fig. 11b). We hypothesize that the composite

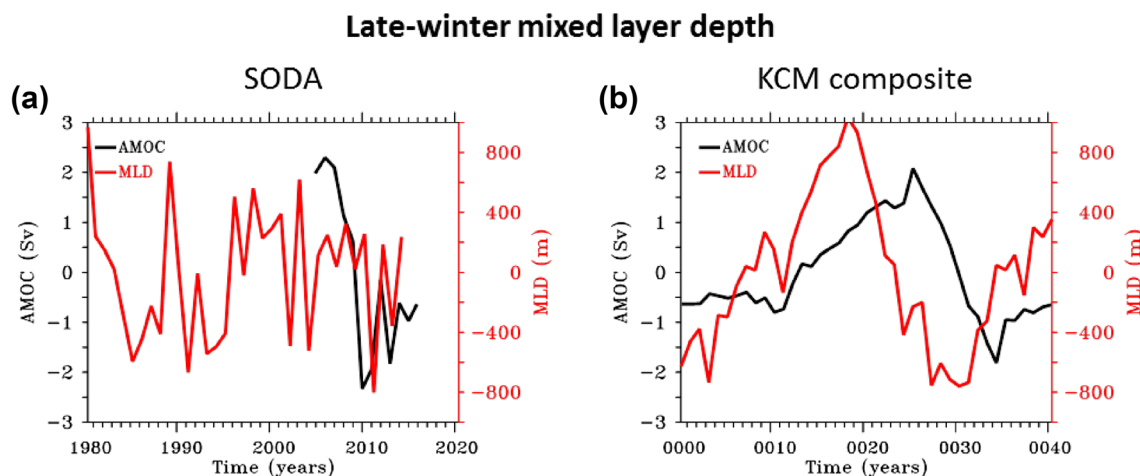


Fig. 11 Late-winter (January–March) maximum mixed layer depth (MLD, m) in the Labrador Sea (70°W – 45°W , 55°N – 70°N) from **a** SODA ocean reanalysis and **b** the composite-evolution from the

KCM. The red curves depict the MLD, and the black curves the AMOC index (as in Fig. 1)

evolution of the MLD in the KCM is due to both diminishing oceanic heat loss at the surface and upper-ocean salt content, as has already been suggested by the contributions of salinity and temperature to the density change at mid-depth (Fig. 9d, f). This view also is supported by the time lag between the Labrador Sea MLD and the AMOC index: whereas the oceanic heat loss would argue for a relatively long time lag of at least a decade (Figs. 9f, 10b), the upper-ocean salt content would support a time lag of only a few years (Figs. 9d, 10f). The MLD leads the AMOC index with a time lag that is between these two time lags, which presumably is the result of the two different timescales involved in changing the Labrador Sea density (Fig. 9d, f).

4 Summary and discussion

We have analyzed a large number of decadal AMOC slowing events simulated in a multi-millennial preindustrial control integration of the KCM and investigated to which extent the recently observed decadal AMOC decline could have been due to internal variability. The analysis was augmented by preindustrial control and historical simulations with 15 climate models participating in the CMIP5. We find that the recently observed AMOC decline is still within the range of the models' internal variability, but it would constitute an extreme realization of such variability provided the models exhibit realistic levels of decadal AMOC variability. In fact the observed decadal AMOC decline exceeds the two-sigma range of the model events. We note that there is some evidence that the CMIP5 models may underestimate internal low-frequency variability in SAT over the North Atlantic (e.g. Cheung et al. 2017). The reasons for

the underestimation are unclear, but one possibility for the failure in simulating realistic levels of SAT variability could be biases in AMOC variability. A number of CMIP5 models underestimate AMOC variability on interannual time scales and therefore may also underestimate variability on longer time scales (Roberts et al. 2014). The KCM as well underestimates interannual AMOC variability (not shown).

We derived the mechanism underlying strong decadal AMOC declines in the KCM. The following mechanism for the development of strong decadal AMOC slowing events is suggested, which involves two factors. First, a rise in SLP over the central and eastern mid-latitude North Atlantic prior to the decadal AMOC slowing reduces the oceanic heat loss over the Labrador Sea. During the following years, the related density signal propagates down to a depth of about 2 km. Second, changes in the horizontal ocean circulation, implied by changes in SSH and upper-ocean heat content, is important. The change in the ocean circulation, which develops with a time delay of a few years in response to the change in low-level atmospheric circulation, reduces the salt content of the upper (0–700 m) Labrador Sea. Both reduced oceanic heat loss and diminished salt content change the density at mid-depth, which weakens Labrador Sea deep convection and in turn slows the AMOC. The northward oceanic heat transport also weakens, giving rise to anomalously cold SST in the central and eastern mid-latitude North Atlantic. We find some evidence for this model-derived mechanism from observations and data from ocean analysis/reanalysis during the recent decadal AMOC slowing event, but the data are rather noisy.

The mechanism outlined in this study is a stochastic one: random and persistent atmospheric high SLP anomalies over the North Atlantic drive decadal AMOC slowing

events. This is supported by spectra computed from North Atlantic SLP time series which are consistent with white noise (not shown). In this picture, the ocean is a slave to the atmosphere and responds with a time delay to low-frequency low-level atmospheric circulation variability.

The implications of this study are twofold. First, major decadal AMOC slowing events can be produced internally in climate models. Assuming that the models simulate realistic levels of decadal AMOC variability, the recently observed decadal slowing would represent an extreme realization of internal variability. This would argue for a relatively high probability that anthropogenic forcing could have played an important role in the observed decadal AMOC slowing event. On the other hand, it may well be possible that climate models underestimate the level of decadal AMOC variability, which would increase the probability of the occurrence of decadal AMOC slowing events with magnitude comparable to that recently observed. Analysis of state-of-the-art global-ocean reanalysis suggest that the recent observed decrease in the AMOC is part of decadal variability of the North Atlantic and can be understood as a recovery from earlier strengthening (Jackson et al. 2016). The decadal AMOC decline has been arrested during the recent years (Smeed et al. 2018). Further, Yashayaev and Loder (2016) report that winter convective overturning in the Labrador Sea reached the deepest aggregate maximum depth since 1994. Thus the recent decadal AMOC decline may well prove to be part of a decadal oscillation. In line with some previous studies, this study also suggests that multi-decadal observational records are required to reliably detect an anthropogenic AMOC slowing.

Second, AMOC variability on the relatively short decadal timescale may significantly influence the surface climate in the North Atlantic sector, which is important to multiyear climate predictability in this region. Most studies so far have highlighted AMOC influences on North Atlantic sector surface climate on multi-decadal timescale and beyond. The type of decadal AMOC variability described here appears to be potentially predictable, as it can be understood as the delayed oceanic response to multiyear changes in the low-level atmospheric circulation, and suitably initialized climate models may hold great potential to forecast associated surface climate variability in the North Atlantic sector.

This study emphasizes internal AMOC variability but does not rule out the possibility that external forcing played a major role during the recent decadal AMOC decline, such as an enhanced meltwater input from the Greenland ice sheet in response to anthropogenic global warming (Yang et al. 2016).

Acknowledgements This study was supported by the BMBF's project "RACE II" and by the InterDec project "The potential of seasonal-to-decadal-scale inter-regional linkages to advance climate predictions"

of the JPI CLIM Belmont-Forum. The climate model integrations were performed at the Computer Centre at the Kiel University and at the High Performance Computing Centre (HRLN).

References

- Barnston AG, Livezey RE (1987) Classification, seasonality and persistence of low-frequency atmospheric circulation patterns. *Mon Weather Rev* 115:1083–1126
- Bindoff NL et al (2013) Climate change 2013. In: Stocker TF et al (eds) *The physical science basis*. Cambridge University Press, Cambridge, pp 867–952
- Booth BB, Dunstone NJ, Halloran PR, Andrews T, Bellouin N (2012) Aerosols implicated as a prime driver of twentieth-century North Atlantic climate variability. *Nature* 484:228–232
- Bryden HL, King BA, McCarthy GD, McDonagh EL (2014) Impact of a 30% reduction in Atlantic meridional overturning during 2009–2010. *Ocean Sci* 10:683–691
- Caesar L, Rahmstorf S, Robinson A, Feulner G, Saba V (2018) Observed fingerprint of a weakening Atlantic Ocean overturning circulation. *Nature* 556:191–196
- Cheng W, Chiang JCH, Zhang D (2013) Atlantic meridional overturning circulation (AMOC) in CMIP5 models: RCP and historical simulations. *J Clim* 26:7187–7197
- Cheung AH et al (2017) Comparison of low-frequency internal climate variability in CMIP5 models and observations. *J Clim* 30:4763–4776
- Cunningham SA et al (2013) Atlantic Meridional Overturning Circulation slowdown cooled the subtropical ocean. *Geophys Res Lett* 40:6202–6207
- Delworth TL, Zeng F (2012) Multicentennial variability of the Atlantic meridional overturning circulation and its climatic influence in a 4000 year simulation of the GFDL CM2.1 climate model. *Geophys Res Lett* 39:L13702. <https://doi.org/10.1029/2012gl052107>
- Delworth TD, Manabe S, Stouffer RJ (1993) Interdecadal variations of the thermohaline circulation in a coupled ocean–atmosphere model. *J Clim* 6:1993–2011
- Dima M, Lohmann G (2010) Evidence for two distinct modes of large-scale ocean circulation changes over the last century. *J Clim* 23:5–16
- Drijfhout S, van Oldenborgh GJ, Cimadoribus A (2012) Is a decline of AMOC causing the warming hole above the North Atlantic in observed and modeled warming patterns? *J Clim* 25:8373–8379
- Goddard PB, Yin J, Griffies SM, Zhang S (2015) An extreme event of sea-level rise along the Northeast coast of North America in 2009–2010. *Nat Commun* 6:6346
- Handmann P et al (2018) The deep western boundary current in the Labrador sea from observations and a high-resolution model. *J Geophys Res Oceans* 123:2829–2850. <https://doi.org/10.1002/2017JG013702>
- Hurrell JW (1995) Decadal trends in the North Atlantic Oscillation: regional temperatures and precipitation. *Science* 269:676–679
- Iwi AM, Hermanson L, Haines K, Sutton RT (2012) Mechanisms linking volcanic aerosols to the Atlantic meridional overturning circulation. *J Clim* 25:3039–3051
- Jackson LC, Peterson KA, Roberts CD, Wood RA (2016) Recent slowing of Atlantic Overturning Circulation as a recovery from earlier strengthening. *Nat Geosci* 9:518–522
- Jung T, Vitart F, Ferranti L, Morcrette JJ (2011) Origin and predictability of the extreme negative NAO winter of 2009/10. *Geophys Res Lett* 38(7):2. <https://doi.org/10.1029/2011gl046786>
- Levermann A, Griesel A, Hofmann M, Montoya M, Rahmstorf S (2005) Dynamic sea level changes following changes in the thermohaline circulation. *Clim Dyn* 24:347–354

- McCarthy GD et al (2015a) Measuring the Atlantic Meridional overturning circulation at 26°N. *Prog Oceanogr* 130:91–111
- McCarthy GD, Haigh ID, Hirschi JJ-M, Grist JP, Smeed DA (2015b) Ocean impact on decadal Atlantic climate variability revealed by sea-level observations. *Nature* 521:508–510
- Nigam S, Ruiz-Barradas A, Chafik L (2018) Gulf Stream excursions and sectional detachments generate the decadal pulses in the Atlantic multidecadal oscillation. *J Clim* 31(7):2853–2870
- Park W, Latif M (2008) Multidecadal and multicentennial variability of the meridional overturning circulation. *Geophys Res Lett* 35:L22703. <https://doi.org/10.1029/2008gl035779>
- Park W, Latif M (2012) Atlantic meridional overturning circulation response to idealized external forcing. *Clim Dyn* 29:1709–1726
- Park W, Keenlyside N, Latif M, Ströh A, Redler R, Roeckner E, Madec G (2009) Tropical pacific climate and its response to global warming in the Kiel climate model. *J Clim* 22(1):71–92. <https://doi.org/10.1175/2008jcli2261.1>
- Park T, Park W, Latif M (2016) Correcting North Atlantic sea surface salinity biases in the Kiel Climate Model: influences on ocean circulation and Atlantic Multidecadal Variability. *Clim Dyn* 47:2543–2560
- Pohlmann H et al (2013) Predictability of the mid-latitude Atlantic meridional overturning circulation in a multi-model system. *Clim Dyn* 41:775–785
- Reintges A, Martin T, Latif M, Keenlyside NS (2017) Uncertainty in twenty-first century projections of the Atlantic Meridional Overturning Circulation in CMIP3 and CMIP5 models. *Clim Dyn* 49:1495–1511
- Ritz SP, Stocker TF, Grimalt JO, Menviel L, Timmermann A (2013) Estimated strength of the Atlantic overturning circulation during the last deglaciation. *Nat Geosci* 6:208–212
- Roberts CD, Jackson L, McNeill D (2014) Is the 2004–2012 reduction of the Atlantic meridional overturning circulation significant? *Geophys Res Lett* 41:3204–3210
- Robson J, Hodson D, Hawkins E, Sutton R (2013) Atlantic overturning in decline? *Nat Geosci* 7:2–3
- Robson J, Ortega P, Sutton R (2016) A reversal of climatic trends in the North Atlantic since 2005. *Nat Geosci* 9:513–517
- Saba VS et al (2016) Enhanced warming of the Northwest Atlantic Ocean under climate change. *J Geophys Res Oceans* 121:118–132
- Schmittner A, Latif M, Schneider B (2005) Model projections of the North Atlantic thermohaline circulation for the 21st century assessed by observations. *Geophys Res Lett* 32:L23710. <https://doi.org/10.1029/2005gl024368>
- Smeed DA et al (2014) Observed decline of the Atlantic Meridional Overturning Circulation 2004 to 2012. *Ocean Sci* 10:39
- Smeed et al (2018) The North Atlantic Ocean is in a state of reduced overturning. *Geophys Res Lett* 45:1527–1533
- Srokosz MA, Bryden HL (2015) Observing the Atlantic Meridional Overturning Circulation yields a decade of inevitable surprises. *Science* 348:1255575
- Sun B, Yu L, Weller RA (2003) Comparison of surface meteorology and turbulent heat fluxes over the Atlantic NWP model analyses versus moored buoy observations. *J Clim* 16:679–695
- Sutton RT, Hodson DLR (2005) Atlantic ocean forcing of North American and European summer climate. *Science* 309:115–118
- Swingedouw D et al (2015) Bidecadal North Atlantic ocean circulation variability controlled by timing of volcanic eruptions. *Nat Commun* 6:6545
- Taylor KE, Stouffer RJ, Meehl GA (2012) An overview of CMIP5 and the experiment design. *Bull Am Meteorol Soc* 93:485–498
- Yang Q et al (2016) Recent increases in Arctic freshwater flux affects Labrador Sea convection and Atlantic overturning circulation. *Nat Commun* 7:13545
- Yashayaev I, Loder JW (2016) Recurrent replenishment of Labrador Sea Water and associated decadal-scale variability. *J Geophys Res Oceans* 121:8095–8114
- Zhang R et al (2013) Have aerosols caused the observed Atlantic multidecadal variability? *J Atmos Sci* 70(4):1135–1144. <https://doi.org/10.1175/jas-d-12-0331.1>

Publisher's Note Springer Nature remains neutral with regard to jurisdictional claims in published maps and institutional affiliations.